ADSORPTION REMOVAL OF ERIOCHROME BLACK T (EBT) AND ROSE BENGAL (RB) FROM AQUEOUS SOLUTIONS USING BIO-SORBENTS COMBINATION

Miada Benkartoussa[1, ✉], Mossaab Bencheikh Lehocine[1], Sihem Arris[1],
Hassen Abdeslam Meniai[1]

Abstract. Adsorption of eriochrome black T (EBT) and rose bengal (RB) mixture from aqueous solutions was investigated using a mixture of low-cost biosorbents – 50 % of raw state potato peels and 50 % of raw state eggshell (M 50%). The surface charge distribution was determined by acid-base titration and the point of zero charge of the M 50% was found to be 8.5. The adsorbent materials were characterized by Fourier transform infrared spectroscopy and X-ray diffraction. It was confirmed that M 50% was mainly composed of calcite and cellulose. The effect of various operating parameters such as contact time, pH, temperature, *etc*., was studied. The amount of the adsorption decreased when solution pH increased. The pseudo-second order kinetic model provided the best fit to the experimental data for the adsorption of EBT and RB. The obtained thermodynamic parameters indicate that the adsorption process is endothermic one. According to the obtained results, the new biosorbent may be recommended as an industrial adsorbent for the treatment of effluents containing EBT and RB.

Keywords: dye, combination, adsorbent, valorize.

1. Introduction

In several industries like textile, paper, food, plastic, leather, *etc*. synthetic dyes have been widely used. The varieties of the dyes are: acidic, reactive, basic, azo, and diazo [1]. These dyes are non-biodegradable due to their toxic nature [2], the elimination of pollutants and colored effluents from wastewater is important for protecting public health and the environment [3]. There are many traditional techniques applied in the dye removal such as coagulation, flocculation, photo degradation, sedimentation [4], ion exchange, and membrane filter processes such as micro- and ultra-filtration and reverse osmosis. These methods are expensive, use chemical products and generate large amounts of sludge [5]. Among these methods, adsorption is superior to other techniques, which are used on industry scale and are environmentally friendly [6]. Because of its low cost and simplicity adsorption has made an important advance in the elimination of colored effluents [7]. The development of new adsorbents, free and abundant, which compete with an expensive adsorbents, such as activated carbon granules or powder, encourages the use of these free biosorbents as an effective solution [8]. A number of these adsorbents are reported in the literature, like fly ash, sawdust, lignite, rice husk, banana pit, potato peels, raw state, and eggshells [2, 7]. The extent of dye removal depends upon the kind of dye, nature of adsorbent and experimental conditions [9].

In reality the colored effluents are in the form of a mixture of dyes, so in the present work, a study was made for the mixture of two dyes: eriochrome black T (EBT) and rose bengal (RB) by raw state potato peels (PPRS) and raw state eggshells (EGRS) to illustrate the value of these bio-sorbents and their use in dye wastewater treatment. The adsorption of dyes is better on the raw state eggshells, and similar to the adsorbent M 50%: (50% of PPRS + 50% of EGRS) but low on raw state potato peels. So, the raw state potato peel was estimated by the addition of the raw state eggshells, because the addition of EGRS on PPRS (M 50%) has to increase the adsorption capacity of PPRS compared to this adsorbent alone, the M 50% was chosen for the following works. Several parameters of the adsorption phenomenon will also be discussed, such as: pH, effect of ionic strength, adsorption kinetics models, *etc*., not forgetting chemical analysis of adsorbents and characterization of adsorbent materials.

[1] Environmental Process Engineering Laboratory (LIPE),
Department of Environmental Engineering,
University Salah Boubnider, Constantine, Algeria
✉ *mbenkartoussa@yahoo.fr*

2. Experimental

2.1. Preparation of Adsorbents

2.1.1. Adsorbents at raw state

Potato peels and eggshells were washed with distilled water and cut into small parts, and then dried at 333 K for 3 days. The obtained product was crushed into granules, sieved to the particle size of 0.315 mm with sifter (ANALYSENSIEB- RETSH-5657 HAANW) and stored in desiccators.

- PPRS: raw state potato peels, EGRS: raw state eggshell

2.1.2. Adsorbent mixture

The biosorbents mixture contained raw state potato peels (PPRS) and raw state eggshell (EGRS) with different proportions, as follows:

- M 25% = 25% of EGRS + 75% of PPRS
- M 50% = 50% of EGRS + 50% of PPRS
- M 75% = 75% of EGRS +25% of PPRS

2.2. Chemical Analyses of Adsorbents

100 mg of adsorbent was placed in 10 ml of 0.1M NaCl solution. The suspension was shaken for 3 days. The solution was then filtered to determine the pH_{cont}. NaCl is a carrier electrolyte allowing to make the migration current of the species negligible in front of diffusion, so the measurement of pH is more stable.

The pH point of zero charge (pH_{pzc}) for the adsorbents were determined by adding 100 mg of adsorbent to four solutions 0.1 M NaCl (20 ml), which initial pH is close to the $pH_{cont,}$ which has been measured and adjusted with NaOH or HCl. The solutions were shaken for 24 h. The pH_{pzc} corresponds to the value of pH when there is no change of this parameter after contact with adsorbent [10]. At the solution $pH_{pzc} > pH$, the support surface is positively charged, when $pH_{pzc} < pH$, the surface will be negative [11].

2.3. Analyses

FT-IR spectrometer BRUKER was used to know various functional groups of the adsorbent using potassium bromide disk method, the FT-IR spectra were recorded at 5000–500 cm^{-1} [11]; X-ray diffraction (XRD) data were obtained by a diffractometer X Pert Pro Panalytical, XRD was used to know the nature and structure of crystallized adsorbent [12].
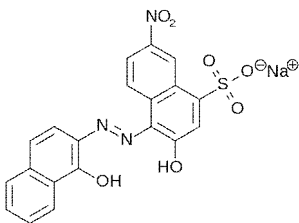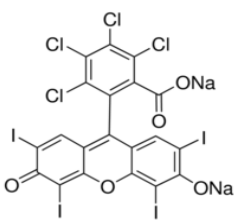
2.4. Adsorbates Properties

The chemical properties and structures of eriochrome black T (EBT) and rose bengal (RB) are presented in Table 1.

The dye solution was prepared by dissolving a mass of dye powder in a known volume of distilled water.

Table 1

Characteristics of EBT and RB

Characteristics	EBT	RB
IUPAC name	Sodium 1-[1-Hydroxynaphthylazo]-6-nitro-2-naphthol-4-sulfonate	4,5,6,7-Tetrachloro-3',6'-dihydroxy-2',4',5',7'-tetraiodo-3*H*-spiro[isobenzofuran-1,9'-xanthen]-3-one
Type of dye	Anionic (acid) azo dye	Anionic (acid) azo dye
Chemical formula	$C_{20}H_{12}N_3NaO_7S$	$C_{20}H_2Cl_4I_4Na_2O_5$
Molecular structure		
Molecular weight, g/mol	461.38	1017.64
Max. wavelength, nm	531	541
Solubility in water at 293 K, g/l	50.0	–
Solubility in ethanol at 293 K, g/l	2.0	–
Color	black	–
The commercial origin	Merck (Germany)	Biochem, Chemopharma (Quebec)

2.5. Batch Mode Adsorption

The study of adsorption was carried out in batch to determine the adsorption of RB and EBT on M 50%. Tests were performed by agitating adsorbents and dye solutions with different initial concentrations (12.5–90 mg/l). Mixing was ensured with the agitation speed of 500 rpm for 15–120 min at 293±2 K. After the equilibrium, the suspension was filtered with a 0.2 μm millipore filter and analyzed using a Jasco V-630 spectrophotometer and *via* a standard calibration curve. The effect of contact time and pH was studied. The pH of the suspension in the experiments was adjusted with 0.1M NaOH or 0.1M HCl. The amount of EBT or RB adsorbed onto M 50% and the removal efficiency R were respectively calculated using the following equations:

$$q = \frac{(C_0 - C)}{m}V \tag{1}$$

$$R = \frac{(C_0 - C)}{C_0} \cdot 100 \tag{2}$$

where C_0 and C are the dye initial concentration and concentration at time t, respectively, mg/l; V is the dye solution volume, l; m is the adsorbent mass, g.

2.6. Adsorption Kinetics Models

Adsorption kinetics is essential in process design since it determines the rate of retention and the necessary time to achieve a certain amount of removal.

2.6.1. Pseudo-first order model

It has been assumed in this model that the sorption rate at instant t is proportional to the difference between the adsorbed quantity at equilibrium (q_e) and time t (q_t), moreover the adsorption is reversible. This model was established by Langeren and Svenska [13]. It can be expressed in a linear form as follows:

$$\frac{dq_t}{dt} = K_1 \cdot (q_e - q_t) \tag{3}$$

where q_e and q_t are the amount of adsorbate adsorbed at equilibrium and time t (min), respectively, mg/g; K_1 is the adsorption rate constant, min^{-1}.

The integration of Eq. (3) for the boundary conditions $t = 0$ to t and $q_t = 0$ to q_t, gives:

$$\ln(q_e - q_t) = \ln q_e - K_1 t \tag{4}$$

The following plot of $\ln(q_e-q_t)$ *vs. t* will give the slope K_1 and the intercept $\ln q_e$.

2.6.2. Pseudo-second order model

The pseudo-second order model is destined for the description of adsorption kinetics in liquid-phase adsorption systems; this model is proposed by Ho and McKay [13]. The linear form of pseudo second order model is expressed as follows:

$$\frac{t}{q_t} = \frac{1}{K_2 \cdot q_{e2}^2} + \frac{1}{q_{e2}}t \tag{5}$$

where K_2 is the adsorption rate constant, $g \cdot mg^{-1} \cdot min^{-1}$.

The linear plot of t/q_t *vs. t* will give $1/q_{e2}$ as slope and $1/K_2 q_{e2}^2$ as the intercept.

2.6.3. The intraparticle diffusion model

The Weber and Moriss model allows the identification of the diffusion mechanism if it is present; the kinetic results were analyzed using the intraparticle diffusion model [14], which is expressed as:

$$q_t = K_{in} t^{0.5} + C_{in} \tag{6}$$

where K_{in} is an intraparticle diffusion constant, $mg/g \cdot min^{0.5}$; C_{in} is the intercept, it is directly proportional to the boundary layer thickness, mg/g.

The linear plot of q_t *vs.* $t^{0.5}$ will give K_{in} as slope and C_{in} as the intercept.

2.7. Isotherm Analyses

2.7.1. Langmuir isotherm

The Langmuir isotherm model is given as Eq. (7) [15]:

$$\frac{1}{q_e} = \frac{1}{q_0} + \frac{1}{q_0 b} \cdot \frac{1}{C_e} \tag{7}$$

where C_e is the concentration of the dye solution at equilibrium, mg/l; q_0 is a practical limiting adsorption capacity; b is the Langmuir constant, l/mg.

2.7.2. Freundlich isotherm

The linear form of the Freundlich equation is:

$$\ln q_e = \ln K_F + \frac{1}{n} \ln C_e \tag{8}$$

where n represents the adsorption intensity and K_F is an indicator of the multilayer adsorption capacity, $mg/g(mg/l)^{1/n}$ [16]. It is usually admitted that values of $n > 1$ proved the favorable adsorption [17].

2.8. Effect of Temperature

The adsorption can be endothermic or exothermic depending on the adsorbent materials and the nature of the adsorbed molecules as well. To understand the thermodynamic phenomenon of EBT and RB adsorption onto M 50% the tests were conducted at the concentration of 25 mg/l and the temperatures ranged from 293 to 353 K. The thermodynamic parameters ΔG, ΔH and ΔS were determined using the following equations:

$$K_d = \frac{q_e}{C_e} \tag{9}$$

$$\Delta G = -RT \ln K_d \tag{10}$$

$$\ln K_d = \frac{\Delta S}{R} - \frac{\Delta H}{RT} \qquad (11)$$

where K_d is the equilibrium constant for adsorption; T is the temperature, K; R is the universal gas constant; ΔG, ΔH, ΔS are Gibbs free energy change, enthalpy and entropy change of the process, respectively.

The values of ΔH, and ΔS are calculated from the slope and intercept of the plot $\ln K_d$ *vs.* $1/T$ [18].

3. Results and Discussion

Removal of anionic dyes EBT and RB by the mixture of adsorbents M 50% from aqueous solution was carried out. Chemical analysis of adsorbents and adsorbents characterization were made. Effect of various parameters such as contact time, pH, ionic strength and temperature, adsorption kinetics models, and isotherm analysis on the adsorption capacity of dyes was studied.

3.1. Adsorbents Characterization

The FT-IR spectrum of the adsorbent M 50% is shown in Fig. 1; the functional groups are presented in Table 2.

According to Fig.1 and Table 2, the peak around 3300 cm^{-1} occurs due to a stretching vibration of the O–H bond in the cellulose, which is part of the PPRS composi-

tion [11]; the peak at 1400 cm^{-1} occurs due to the stretching of the C–O bond in the carbonate CO$_3^{-2}$, an important component of EGRS [19], the remaining picks are identified in Table 2.
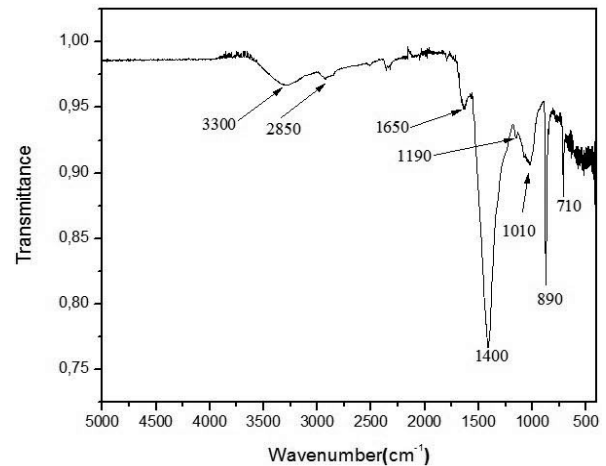

Fig. 1. FT-IR spectrum of M 50%

The XRD pattern for M 50% is presented in Fig. 2. The distinctive peaks of the XRD pattern were identified as the crystalline phase of CaCO$_3$ in the calcite form. It can be seen that the eggshell sample in M 50% is composed of CaCO$_3$ [19].

Table 2

The functional groups of M 50%

| Wavenumber, cm^{-1}	Vibration	Probable groupings	Ref.
3300	stretching	O–H bond related to cellulose	[20], [11]
2850	asymmetric stretching	C–H bond presented in methyl group	[20], [11]
1650	stretching	C=O bond in the secondary amide	[21], [22]
1400	stretching	C–O bond corresponding to the carbonate CO$_3^{-2}$	[19]
1190	stretching	C–O bond related to a lignin	[20], [11]
1010	stretching	C–O–C bond in the cellulose	[11]
890–710	deformation	Due to the out-of-plane and in-plane deformation modes of carbonate	[19]
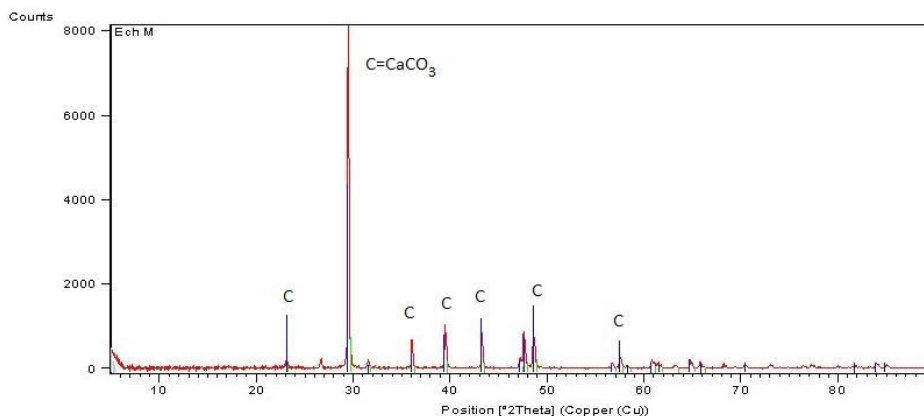
Fig. 2. Typical X-ray diffraction pattern for M 50%

3.2. Effect of Operating Parameters

3.2.1. Effect of contact time

Fig. 3 illustrates the removal efficiency *R* of EBT and RB with the initial concentration of 25 mg/l on different adsorbents (PPRS, EGRS, M 25%, M 50% and M 75%). For EBT and RB, the removal efficiencies using EGRS, M 50% and M 75% have the same value and it is higher compared to PPRS. For example, when EGRS is mixed with PPRS (M 50%) an increase in the removal efficiency is from 35 to 63% for EBT and from 60 to 90 % for RB. The obtained values of the removal efficiencies were close to the EGRS one; the mixture of EGRS and PPRS (M 50%) has to rise the amount of adsorption for the latter one (PPRS). Therefore, the PPRS was considerably valued by the addition of EGRS to PPRS.

Clearly, since, the adsorption process shows the transfer of the pollutant from the liquid phase to the solid one, the contact time between two phases has an effect on the mass transfer rate. Consequently, it is important to study its effect on the capacity of retention by M 50% (Fig. 3).

This variation shows clearly that the curves are of a saturation type and the chemical equilibrium was attained for EBT and RB after 80 and 20 min, respectively; during the adsorption of RB, the saturation curves rises sharply in the initial stages, indicating that there are a great number of readily accessible vacant sites in biosorbent M 50% [23], unlike for EBT, there is a phenomenon of filling layer by layer. Therefore, an equilibrium time of 120 min was assumed for all further experimental runs.

3.2.2. Effect of pH

The solution pH is important for its effect on the adsorbent and sorbate. In this study, the adsorption of EBT and RB on M 50% was carried within pH from 3.01 to 11.75.

Fig. 4 shows the obtained results. When EBT pH increases from 3.01 to 5.3 the adsorption capacity raises from 2.4 to 2.6; while pH varies from 5.3 to 8.65 the adsorption capacity decreases from 2.6 to 1.7; the adsorption capacity is not change with the variation of pH from 8.65 to 11.75 (Fig. 4b).

Fig. 4c [24] shows that EBT is an anionic dye. When pH increases from 3.01 to 5.3 the adsorbent surface charge of M 50% is positive according to pH_{pzc} in Table 3 and Fig. 4d. Therefore, the attraction between the dye and the adsorbent is very important and the amount of adsorption is important as well. For the pH range of 5.3–8.65 the adsorbent surface charge is positive and the coloring solution is overloaded with [OH⁻], so the amount of adsorption will decrease due to the competition between anionic dye (EBT) and [OH⁻] [25]. However, for the pH variation from 8.65 to 11.75 the amount of adsorption did not vary, and this is due to the phenomenon of ion exchange or complexation [26].

Table 3

Characteristics of different adsorbents

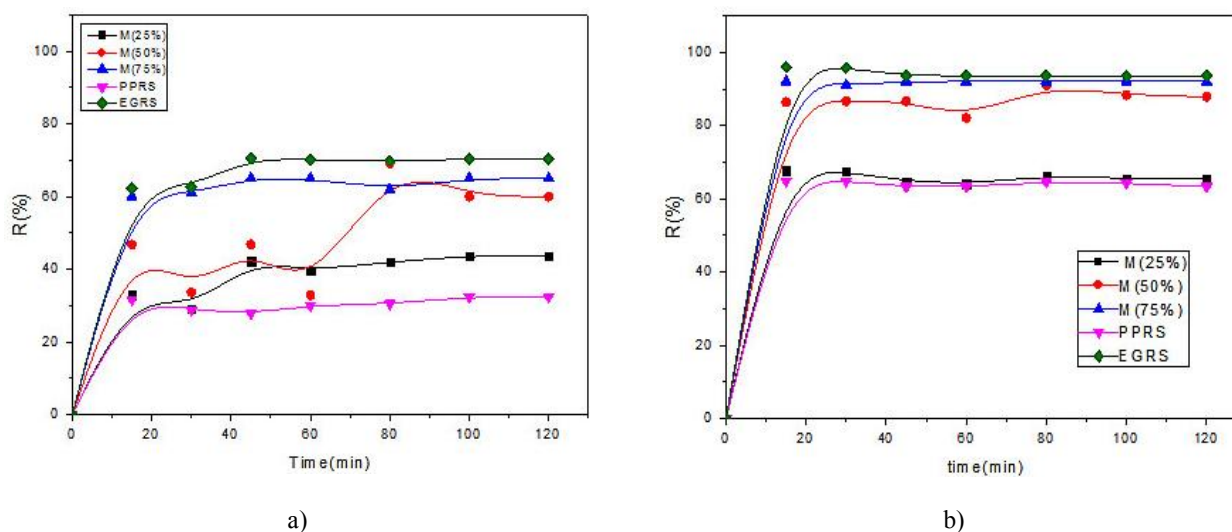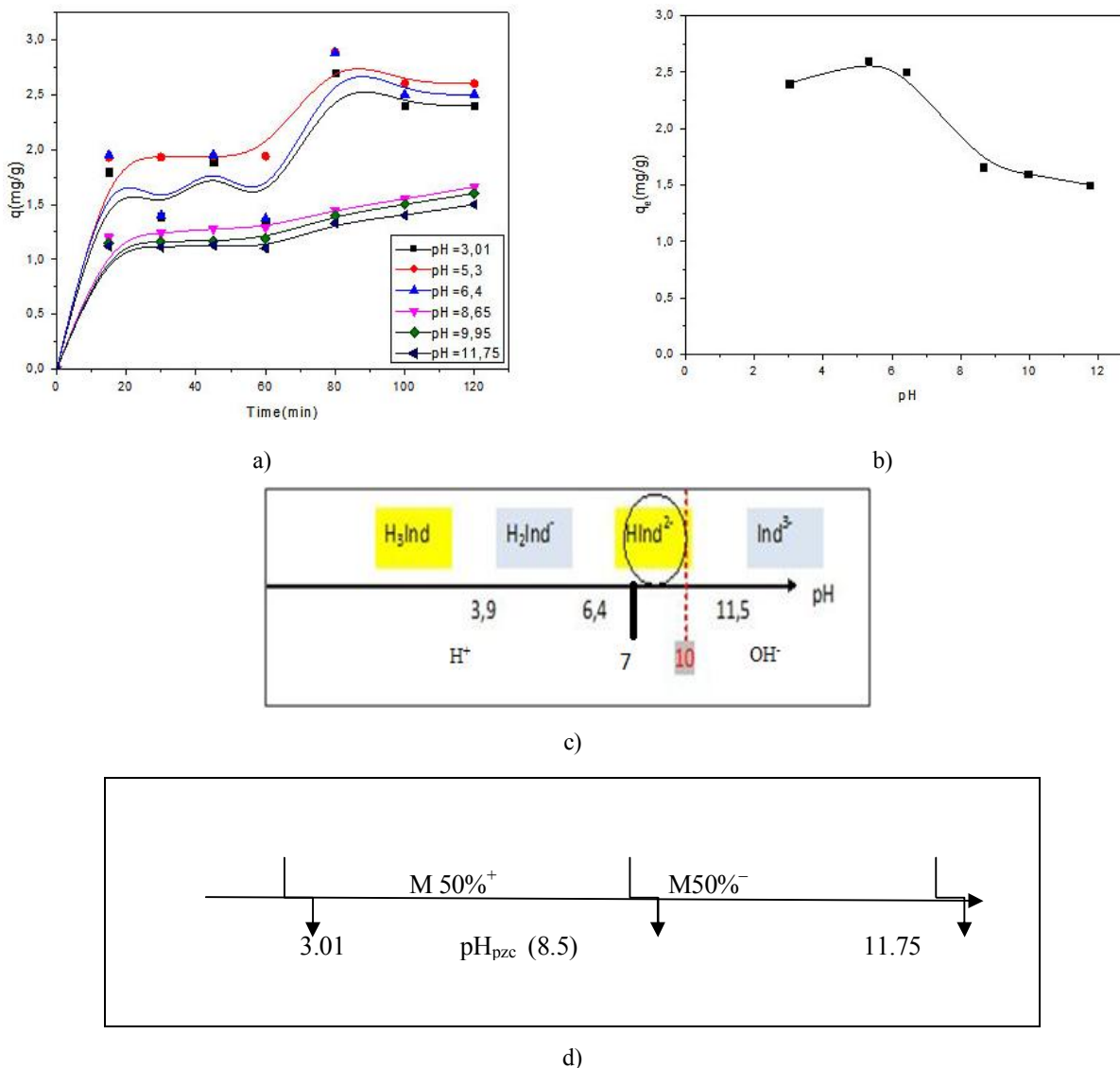| Adsorbent	pH_{cont}	pH_{pzc}
PPRS	8.37	8.06
EGRS	8.28	8.56
M 50%	8.43	8.5

a)

b)

Fig. 3. Effect of contact time on the adsorption of EBT (a) and RB (b).
Conditions: $C_0 = 25$ mg/l, stirring speed = 500 rpm, sorbent dosage = 0.6 g (100 ml⁻¹), $T = 293 \pm 2$ K, pH = 6.4, $d < 0.315$ mm

a)

b)

c)

d)

Fig. 4. Effect of pH on EBT (a); pH *vs.* capacity q_e (b); distribution of chemical species of EBT (c); charge of M 50% surface. Conditions: C_0 = 25 mg/l, stirring speed = 500 rpm, sorbent dosage = 0.6 g (100 ml^{-1}), T = 293±2 K, d < 0.315 mm

According to Fig. 5b the increase in pH from 3.01 to 11.75 for RB decreases the amount of adsorption from 3.83 to 2.6. The RB is an anionic dye [27]. When pH increases, the adsorbent surface charge became more and more negative, so the repulsive forces between the dye and adsorbent became more important, resulting in a decreased adsorption [25].

3.2.3. Effect of ionic strength

The effect of ionic strength on adsorption has been investigated in this work. It was studied by the addition of NaCl or ZnCl$_2$ in the colored solution of EBT and RB (25 mg/l) at different concentrations (0.1M and 0.3M).

The addition of salt increases considerably the adsorbed amount of dyes from 1.17 to 20 mg/g for EBT

and from 1.82 to 25 mg/g for RB (Fig. 6), it can be attributed to the aggregation of dye molecules induced by the action of salt ions (NaCl or ZnCl$_2$) and the decrease of mutual repulsive forces between the dye and the adsorbent [28].

3.2.4. Adsorption kinetics models

The plot of ln(q_e–q_t) *vs. t*, for both dyes and for the different initial concentrations is shown in Figs. 7a and 8a. Tables 4 and 5 summarize the obtained fitting results. As the difference between experimental q_e and first order simulated q_e is considerable, the obtained correlation coefficient values are very small; consequently the adsorption is not the first order reaction.

a)   b)
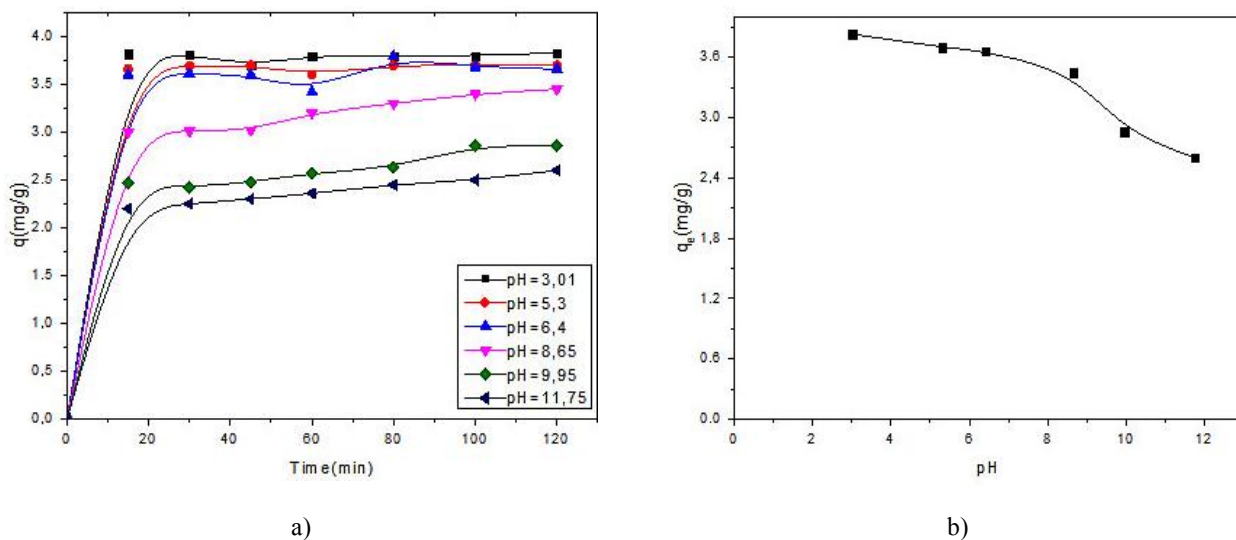
Fig. 5. Effect of pH on RB (a) and variation of pH *vs.* capacity q_e (b).
Conditions: C_0 = 25 mg/l, stirring speed = 500 rpm, sorbent dosage = 0.6 g (100 ml^{-1}), T = 293±2 K, d < 0.315 mm


a)   b)
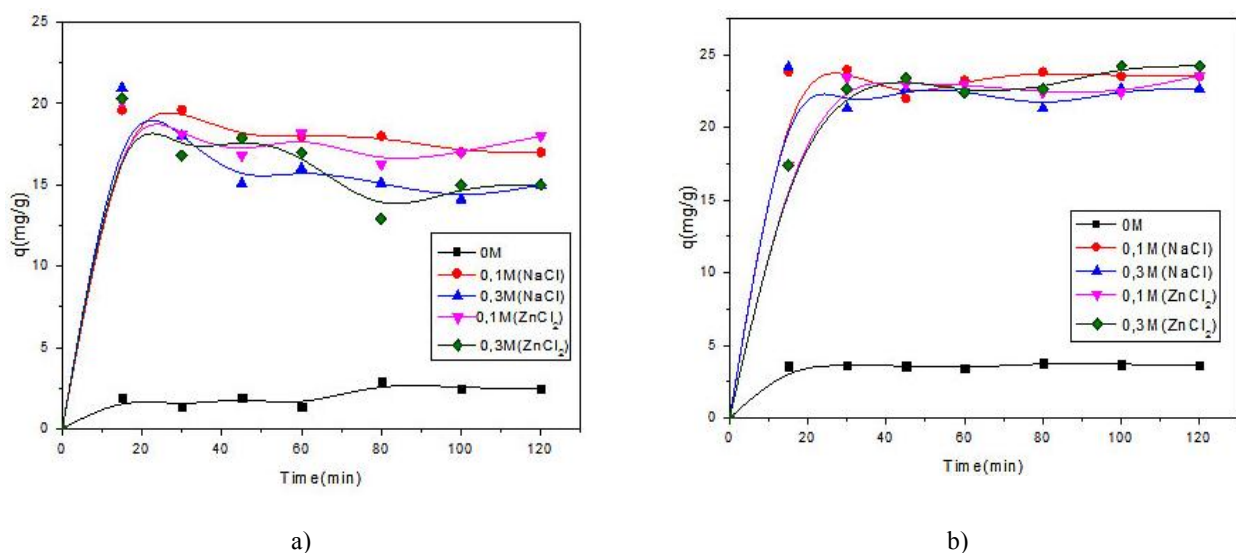
Fig. 6. Effect of EBT (a) and RB (b) ionic strength.
Conditions: C_0 = 25 mg/l, stirring speed = 500 rpm, sorbent dosage = 0.6 g (100 ml^{-1}), T = 293±2 K, pH = 6.4, d < 0.315 mm

Due to the non-applicability of the pseudo-first order model to experimental data, they have been tested with the second order kinetic model by plotting t/q_t *vs. t* (Figs. 7b and 8b). The fitting results are collected in Tables 4 and 5, the rate constant K_2 was found to be decreased from 0.1736 to 0.00813 with the increase in the initial dye concentration from 12.5 to 90 mg/l for RB. Moreover, plot correlation coefficients are closer to one, furthermore, the difference between experimental q_e and second order simulated q_e is insignificant, as given in Table 6 ($C_{0,EBT}$ = 12.5 mg/l, $q_{e,exp}$ = 1.17 mg/g, $q_{e,calc}$ = = 1.33 mg/g). It implies that the adsorption of EBT and

RB on biosorbent M 50% is well described by the pseudo-second order kinetic model.

Figs.7c and 8c show the representation of q_t *vs.* the time square root of the tested concentrations and indicate that the diffusion within the pores is involved in the sorption process but not as the only limiting mechanism. We have two regions: the diffusion in the pores (intraparticle diffusion) and finally the last step which represents the equilibrium (the intraparticle diffusion begins to slow down). The values of C_{in} increase when the concentration raises (Tables 4, 5) [29].
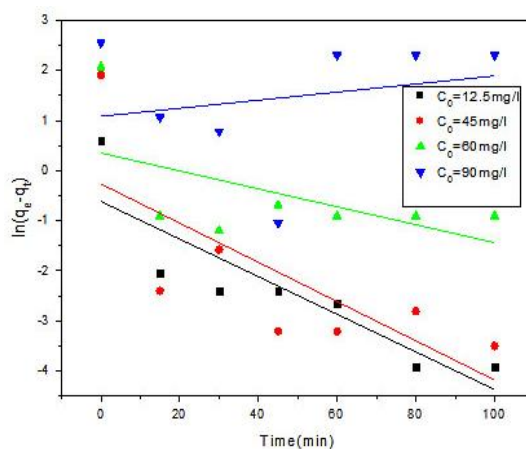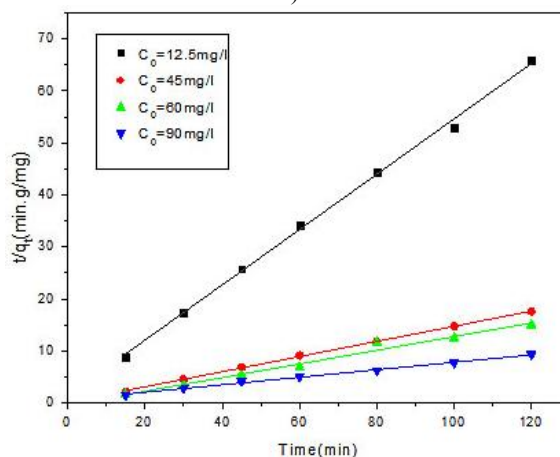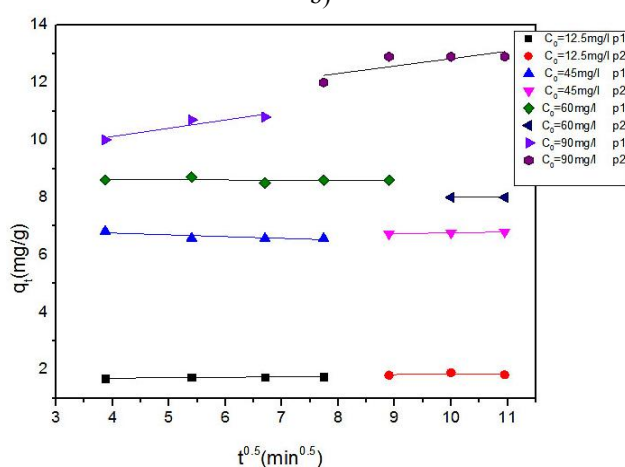
a)

a)

b)

b)

c)
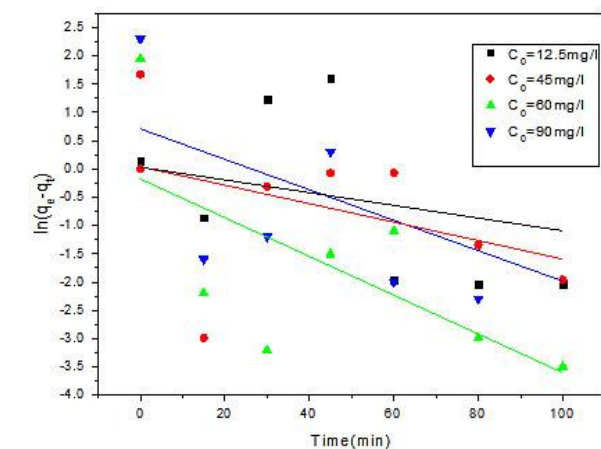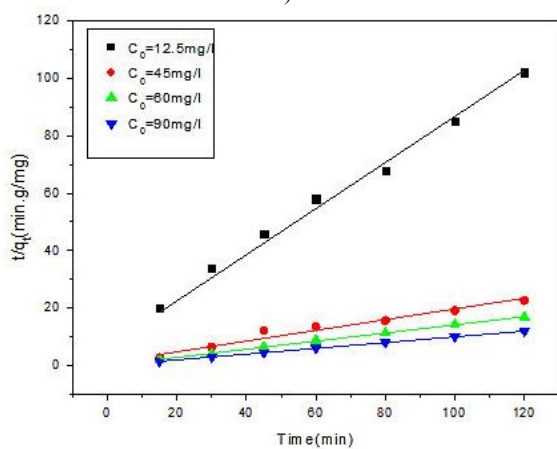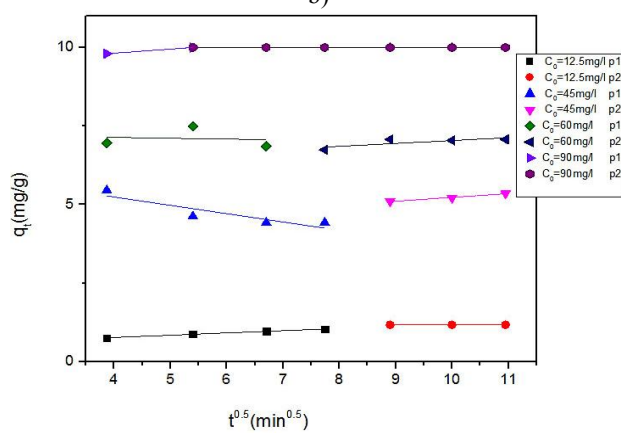
c)

Fig. 7. Adsorption kinetics of EBT: pseudo-first order kinetics (a); pseudo-second order kinetics (b); intraparticle diffusion (c). Conditions: stirring speed = 500 rpm, sorbent dosage = 0.6 g (100 ml^{-1}), T = 293±2 K, pH = 6.4, d < 0.315 mm

Fig. 8. Adsorption kinetics of RB: pseudo-first order kinetics (a); pseudo-second order kinetics (b); intraparticle diffusion (c). Conditions: stirring speed = 500 rpm, sorbent dosage = 0.6 g (100 ml^{-1}), T = 293±2 K, pH = 6.4, d < 0.315 mm

Table 4

Kinetic parameters of EBT adsorption using M 50% at different concentrations

C_0, mg/l	12.5	45	60	90
K_1, min^{-1}	0.033	0.001	0.0328	0.0137
q_e, mg/g	2.0137	1.0565	0.8436	1.03045
R^2	**0.3713**	**0.1785**	**0.4213**	**0.0565**
K_2, g·mg^{-1}·min^{-1}	0.051	0.017	0.3923	0.33
q_{e2}, mg/g	1.3333	5.8823	7.1428	10.0
R^2	**0.9956**	**0.9621**	**0.9985**	**1.0**
K_{in}, mg/g·min$^{0.5}$	0.072	-0.265	-0.026	0.0132
C_{in}, mg/g	0.477	6.298	7.246	9.298
R^2	**0.9930**	**0.8159**	**0.9738**	–
K_{in}, mg/g·min$^{0.5}$	0	0.121	0.095	-1.163 10^{-15}
C_{in}, mg/g	1.17	4.012	6.117	10.0
R^2	–	**0.9921**	**0.6264**	–

Table 5

Kinetic parameters of RB adsorption using M 50% at different concentrations

C_0, mg/l	12.5	45	60	90
K_1, min^{-1}	0.0375	0.03	0.01	-0.008
q_e, mg/g	0.5433	0.7710	0.9900	2.9445
R^2	**0.7821**	**0.5446**	**0.3346**	**0.0448**
K_2, g·mg^{-1}·min^{-1}	0.1736	0.1153	0.04	0.00813
q_{e2}, mg/g	2	7.14	7.69	14.2
R^2	**0.9980**	**0.9994**	**0.9980**	**0.9960**
K_{in}, mg/g·min$^{0.5}$	0.0150	-0.0619	-0.0081	0.0287
C_{in}, mg/g	1.638	7.001	8.658	8.967
R^2	**0.9154**	**0.7040**	**0.2665**	**0.8742**
K_{in}, mg/g·min$^{0.5}$	0.0117	0.0292	0.0	0.0258
C_{in}, mg/g	1.724	6.461	8.0	10.247
R^2	**0.8738**	**0.9982**	–	**0.4510**

Table 6

Comparison between experimental and calculated q_e for EBT and RB

Dye	C_0, mg/l	$q_{e,\,exp}$, mg/g	$q_{e,\,calc}$, mg/g
EBT	12.5	1.17	1.3333
	45	5.35	5.8823
	60	7.07	7.1428
RB	12.5	1.82	2.0
	45	6.79	7.14
	60	8.0	7.69

Table 7

Isotherms constants for EBT and RB adsorption on M 50%

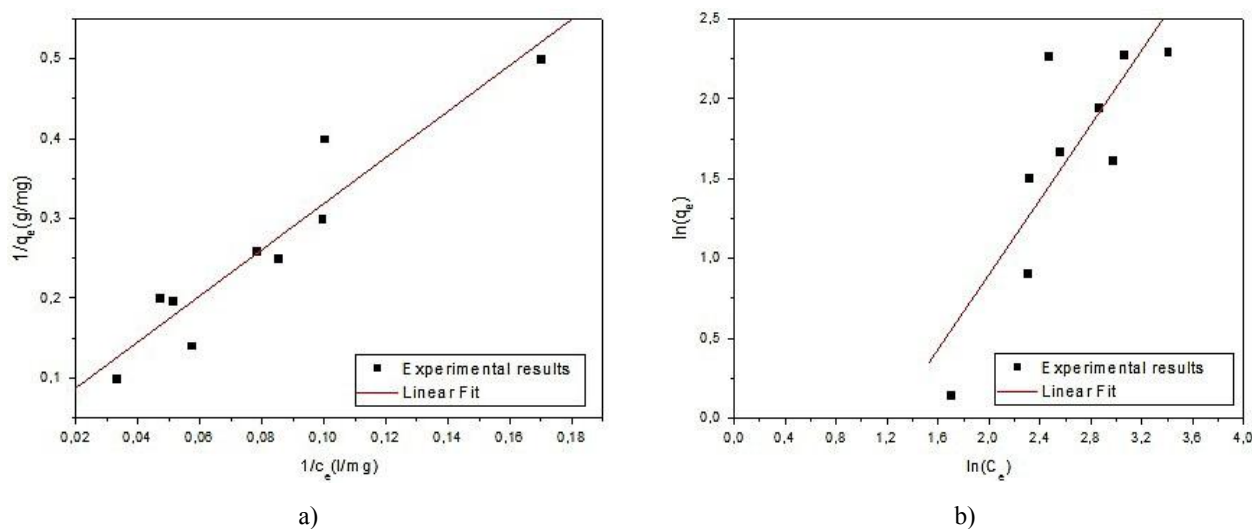| EBT Adsorption on M 50%			RB Adsorption on M 50%	
Models	Constants	R^2	Constants	R^2
Langmuir	q_0 = 34.48 mg/g b = 0.0104 l/mg	**0.8962**	q_0 = 21.2 mg/g b = 0.066(l/mg	**0.9645**
Freundlich	K_F = 0.2364 mg/g(mg/l)$^{1/n}$ n =0.8538	**0.6840**	K_F = 2.7556 mg/g(mg/l)$^{1/n}$ n =1.9261	**0.4057**

Fig. 9. Linear plots of EBT: Langmuir (a) and Freundlich (b) isotherms
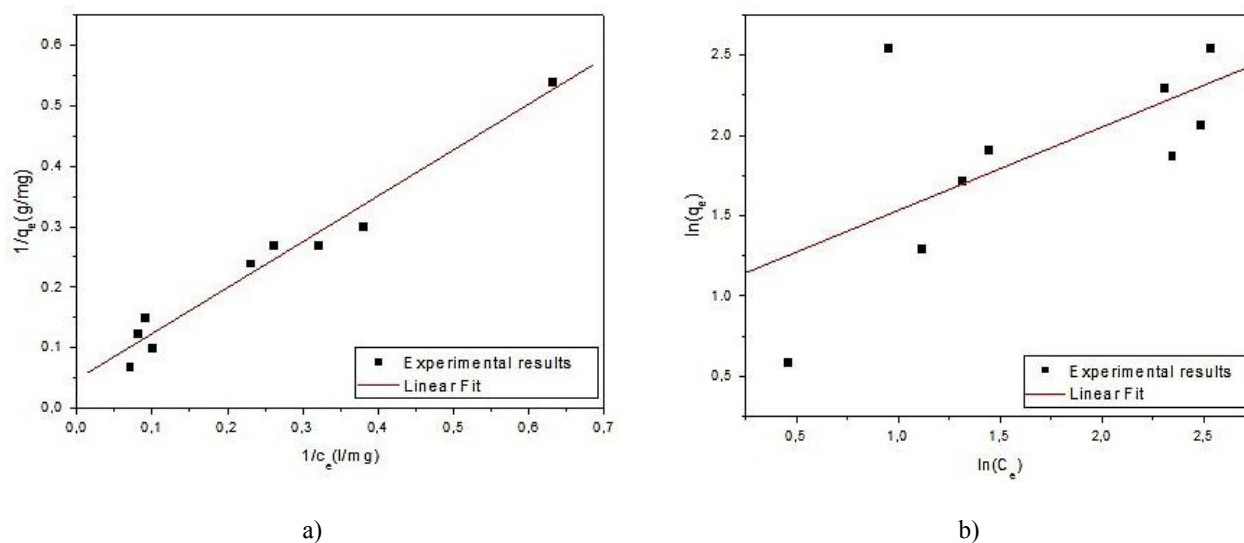

Fig. 10. Linear plots of RB: Langmuir (a) and Freundlich (b) isotherms

3.2.5. Isotherm analysis

The EBT and RB isotherms are shown in Figs. 9 and 10, respectively. The results of this analysis are tabulated in Table 7. It can be seen that the correlation factors R^2 are close to 1 for Langmuir, so the adsorption of EBT and RB on bio-sorbent M 50% is a monolayer adsorption on homogeneous surfaces ($q_0 = 34.48$ mg/g for EBT and $q_0 = 21.2$ mg/g for RB). The value of n_{RB} was more than 1, which proved the favorable adsorption.

The essential features of the Langmuir isotherm can be expressed in terms of a dimensionless constant separation factor R_L [30]:

$$R_L = \frac{1}{(1+bC_0)} \qquad (12)$$

The value of R_L indicates the shape of the isotherms to be: unfavorable ($R_L > 1$), linear ($R_L = 1$), favorable ($0 < R_L < 1$), or irreversible ($R_L = 0$).

The values of R_L observed in Fig. 11 are between 0.5–0.14, indicating that adsorption is favorable. It is noted that when C_0 increases, R_L approaches to zero and the adsorption becomes more favorable at high initial concentrations.

3.2.6. Effect of temperature

Linear plots of EBT and RB thermodynamic parameters are represented in Figs. 12-13 and Table 8. For EBT (according to Table 8) the positive values of ΔG indicate the slow nature of the process [31]. The enthalpy ΔH was found to be positive as well, confirming the endo-

thermic nature of the dye adsorption process within the temperature interval of 293–313 K; the variation of enthalpy ΔH in the interval of 40–120 kJ/mol suggests that the adsorption system may be of chemical nature (chemisorption); the physical sorption is characterized by values of ΔH (< 40 kJ/mol), so the calculated value of 12.31 kJ/mol indicates clearly the physical sorption [32]. The positive value of ΔS reflects the increased randomness of the solid-solution interface [33].

In the case of RB the negative values of ΔG indicate that the process is spontaneous [31]. The enthalpy ΔH is positive confirming the endothermic nature of dye adsorption in the interval of 293–313 K. The value of enthalpy 26.8 kJ/mol indicates that the adsorption of RB on M 50% is a physical sorption [32], the same variation of ΔS for EBT [33].
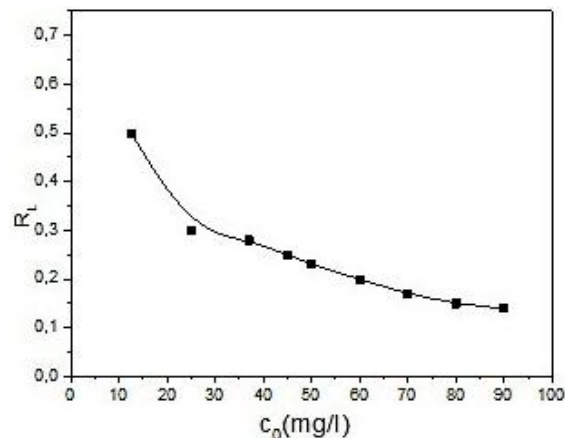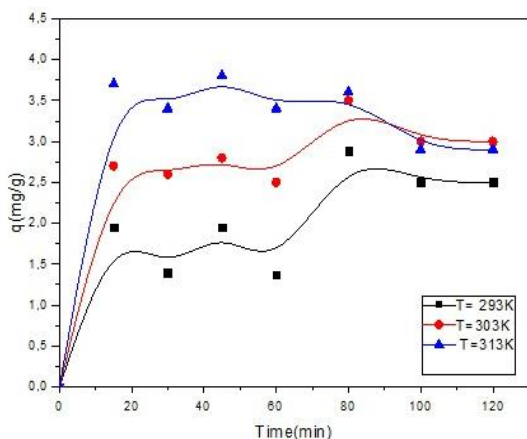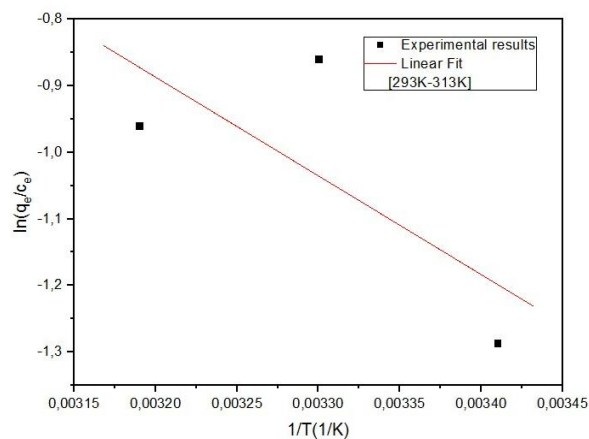

Fig. 11. Separation factor RL of RB adsorption on M 50%

a)   b)

Fig. 12. Temperature effect (a) and linear plot of thermodynamic parameters for EBT. Conditions: $C_0 = 25$ mg/l, stirring speed = 500 rpm, sorbent dosage = 0.6 g (100 ml^{-1}), pH = 6.4, $d < 0.315$ mm
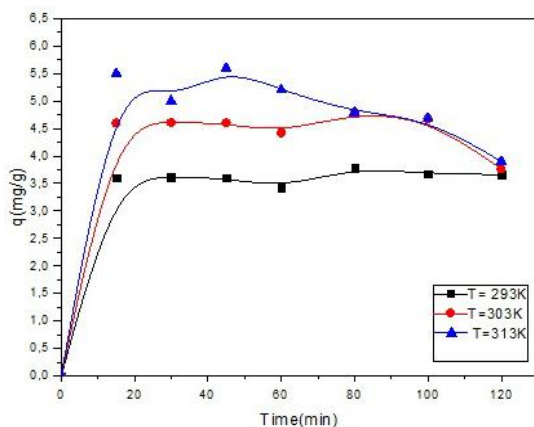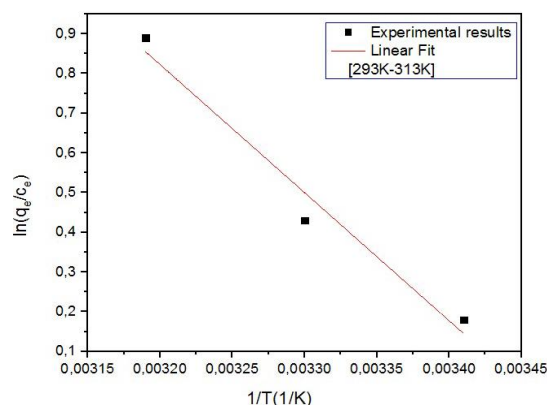

a)   b)

Fig. 13. Temperature effect (a) and linear plot of thermodynamic parameters for RB. Conditions: $C_0 = 25$ mg/l, stirring speed = 500 rpm, sorbent dosage = 0.6 g (100 ml^{-1}), pH = 6.4, $d < 0.315$ mm

Thermodynamic parameters of EBT and RB adsorption on M 50%

Dye	T, K	ΔG, kJ/mol	ΔH, kJ/mol	ΔS, kJ/mol·K
EBT	293	2.93	12.31	0.03199
	303	2.61		
	313	2.29		
RB	293	-0.156	26.8	0.092
	303	-1.076		
	313	-1.99		

4. Conclusions

The results obtained show that M 50% composed of PPRS and EGRS (50:50) is an efficient sorbent for the removal of mixture dyes (EBT, RB) from aqueous solutions. The FTIR and XRD characterization confirmed that M 50% is composed of calcite ($CaCO_3$) and cellulose. The study considered the effect of different physico-chemical parameters on EBT and RB retention such as pH, effect of ionic strength, *etc*. The adsorbed amounts for EBT and RB increased due to the presence of salts. The kinetic study showed that adsorption follows a second order model. The equilibrium results were evaluated according to the Langmuir and Freundlich isotherms. The Langmuir model was found to be in a good agreement with experimental data.

Acknowledgments

References

[1] Gezer B.: Int. J. Agric. For. Life Sci., 2018, **2**, 1.
[2] Benkartoussa Z., Karima B., Mossaab B.: JDOC, 2015, **1**, 10. http://jdoc.sawis.org
[3] Djebbar M., Djafri F.: Chem. Chem. Technol., 2018, **12,** 272. https://doi.org/10.23939/chcht12.02.272
[4] Erguler G.: Miner. Eng., 2015,**76**, 10. https://doi.org/10.1016/j.mineng.2015.02.002
[5] Khademolhosseini M. Mobasherpour I., Ghahremani D.: Chem. Chem. Technol., 2018, **12,** 372. https://doi.org/10.23939/chcht12.03.372
[6] Sabadash V., Mylanyk O., Matsuska O., Gumnitsky J.: Chem. Chem. Technol., 2017, **11**, 459. https://doi.org/10.23939/chcht11.04.459
[7] Benkartoussa M., Lehocine B.: Algerian J. Eng. Res., 2018, **2**, 45.
[8] Shachneva E., Archibasova D.: Chem. Chem. Technol., 2018, **12**, 182. https://doi.org/10.23939/chcht12.02.182
[9] Al Azabi K., Al Marog S., Abukrain A., Sulyman M.: Chem. Res. J., 2018, **3**, 45.
[10] Ekpete O., Horsfall M.: Res. J. Chem. Sci., 2011, **3**, 10.
[11] Gupta N., Kushwaha A., Chattopadhyaya M.: Arabian J. Chem., 2016, **9**, 707. https://doi.org/10.1016/j.arabjc.2011.07.021
[12] Gravereau P.: La diffraction des rayons x par les poudres, ICMCB-CNRS, Université Bordeaux 1, 2012.
[13] Samarghandy M., Hoseinzade E. *et al*.: BioRes., 2011, **6**, 4840.
[14] Weber W.: Physicochemical Processes: for Water Quality Control. Wiley, New York 1972.
[15] Abbas A., Jaafar M., Ismail A.., Wan Sulaiman W.: Chem. Eng. Transact., 2017, **56**, 151. https://doi.org/10.3303/CET1756026
[16] Crini G.: Dyes Pigm., 2008, **77**, 415. https://doi.org/10.1016/j.dyepig.2007.07.001
[17] Nethaji S., Sivasamy A., Mandal A.: Int. J. Environ. Sci. Technol., 2013, **10**, 231. https://doi.org/10.1007/s13762-012-0112-0
[18] Bellir K., Sadok Bouziane I., Boutamine Z. *et al*.: Energy Procedia, 2012, **18**, 924. https://doi.org/10.1016/j.egypro.2012.05.107
[19] Flores-Cano J., Leyva-Ramos R., Mendoza-Barron J. *et al*.: Appl. Surf. Sci., 2013, **276**, 682. https://doi.org/10.1016/j.apsusc.2013.03.153
[20] http://r.chouchi.free.fr/modeles%20moleculaires/frequences.html
[21] Lotfi M.: Cours de Spectroscopie IR, Maitres de conférences classe A, Directeur du laboratoire de recherche LGVRNAQ ,
[22] Taleb H., Chehade Y., Abou Zour M.: Int. J. Electrochem. Sci., 2011, **6**, 6542.
[23] Bousba S., Bougdah N., Messikh N., Magri P.: Phys. Chem. Res., 2018, **6**, 613. https://doi.org/10.22036/pcr.2018.129154.1482
[24] Raclot C.: Dosage des ions Nickel (II) par l'ETDA, concours aggregation interne ,ancient professeur du lycée des haberges 20014 Vesoul France 2011.
[25] Larakeb M., Youcef L., Achour S.: J. New Technol. Mater., 2016, **6**, 19. https://doi.org/10.12816/0043919
[26] Larous S., Meniai A.: Energy Procedia, 2012, **18**, 915. https://doi.org/10.1016/j.egypro.2012.05.106
[27] Nandhakumar V., Rajathi A., Venkatachalam R. *et al*.: SOJ Mater. Sci. Eng., 2015, **1**. https://doi.org/10.15226/sojmse.2016.00121
[28] Alberghina G., Bianchini R., Fichera M., Fisichella S.: Dyes Pigm., 2000, **46**, 129. https://doi.org/10.1016/S0143-7208(00)00045-0
[29] Hameed B., Tan I., Ahmad A.: Chem. Eng. J., 2008, **144**, 235. https://doi.org/10.1016/j.cej.2008.01.028
[30] Hall K., Eagleton L., Acrivos A., Vermeulen T.*:* Ind. Eng. Chem. Fundamen., 1966, **5**, 212. https://doi.org/10.1021/i160018a011
[31] Al-Muhtaseb A., Ibrahim K., Albadarin A. *et al*.: Chem. Eng. J., 2011, **168**, 691. https://doi.org/10.1016/j.cej.2011.01.057
[32] Wu F., Tseng R., Juang R.: Environ. Technol., 2001, **22**, 721. https://doi.org/10.1080/09593332208618235

[33] Belaid K., Kacha S.: J. Water Sci., 2011, **24**, 131.
https://doi.org/10.7202/1006107ar

ВИДАЛЕННЯ ЕРІОХРОМУ ЧОРНОГО Т І БЕНГАЛЬСЬКОГО РОЖЕВОГО З ВОДНИХ РОЗЧИНІВ З ВИКОРИСТАННЯМ СУМІШІ БІОСОРБЕНТІВ

Анотація*. Адсорбцію барвників еріохрому чорного Т (ЕЧТ) та бенгальського рожевого (БР) з водних розчинів проведено з використанням суміші (50:50) недорогих біосорбентів – кожури картоплі та яєчної шкарлупи (М 50%). Кислотно-основним титруванням встановлений розподіл поверхневого заряду, а точка нульового заряду М 50% дорівнює 8,5. Характеристику адсорбентів визначено за допомогою Фур'є-спектроскопії та рентгеноструктурного аналізу. Встановлено, що М 50% переважно складається з кальциту та целюлози. Вивчено вплив різних робочих параметрів, таких як час контакту, рН, температура тощо. Доведено, що адсорбція зменшується з підвищенням рН розчину. Показано, що кінетична модель псевдодругого порядку найкраще узгоджується з експериментальними даними адсорбції ЕЧТ та БР. Отримані термодинамічні параметри вказують на те, що адсорбційний процес є ендотермічним. Рекомендовано використовувати комбінований біосорбент у промисловості для очищення стоків, що містять ЕЧТ та БР.*

Ключові слова*: барвник, комбінація, адсорбент, Фур'є-спектроскопія, рентгеноструктурний аналіз.*